GNSS Integrity Monitoring for Rail Applications: Two-Tiers Method

COSIMO STALLO, Member, IEEE
Consortium RadioLabs, Rome, Italy

ALESSANDRO NERI, Member, IEEE

PIETRO SALVATORI
Consortium RadioLabs, Rome, Italy

ROBERTO CAPUA
Società Generale di Informatica, Rome, Italy

FRANCESCO RISPOLI
Ansaldo STS, Genoa, Italy

This paper presents an innovative global navigation satellite system (GNSS) fault detection and exclusion approach for the adoption of satellite localization in the rail sector. Current global integrity monitoring systems cannot guarantee the safety level needed for such applications as train control where tolerable hazard rate in the order of 10^{-9}/h is required. A new method, named two tiers, enabling to integrate local augmentation systems and global augmentation infrastructures, is presented. It is based on the comparison of single differences residuals among satellites for detecting signal in space (SIS) faults and double difference residuals among local augmentation stations and satellite-based augmentation systems ranging and integrity monitoring stations for detecting reference stations faults. GPS SIS faults described in literature and real GNSS raw data recorded on a train are taken into account. This study reports the performance analysis for the two-tiers approach carried out during relevant European projects. A test-bed architecture has been developed through the implementation of the algorithm in real time on a local augmentation operational center. Relevant performances have been tested on a rail track for validating the algorithm in real operative conditions. Significant results of the analysis are reported for SIS integrity assessment only.

Manuscript received November 27, 2017; revised April 27, 2018 and July 30, 2018; released for publication October 4, 2018. Date of publication October 23, 2018; date of current version August 7, 2019.

DOI. No. 10.1109/TAES.2018.2876735

Refereeing of this contribution was handled by M. Joerger.

This work was supported by Lazio INNOVA of Lazio Region under Contract VIRGILIO (Virtual InsttRuments for GNSS AugmentatIon and LocalizatIOn)-LR 13/2008.

Authors' addresses: C. Stallo and P. Salvatori are with Consortium RadioLabs, 00198 Rome, Italy, E-mail: (cosimo.stallo@radiolabs.it; pietro.salvatori@radiolabs.it); A. Neri is with the Engineering Department, University of Roma TRE, 00146 Roma, Italy, and also with RadioLabs Consortium, 00198 Rome, Italy, E-mail: (alessandro.neri@uniroma3.it); R. Capua is with Società Generale di Informatica, 00143 Rome, Italy, E-mail: (rcapua@sogei.it); F. Rispoli is with Ansaldo STS, 16151 Genoa, Italy, E-mail: (francesco.rispoli@ansaldo-sts.com). *(Corresponding author: Cosimo Stallo.)*

I. INTRODUCTION

According with [1]–[3], the introduction of global navigation satellite systems (GNSS) technology for localizing a train and the adoption of Internet protocol (IP)-based communications are the next frontiers for the European standard for train control: European railway traffic management system (ERTMS)/European train control system. Major benefits of such innovations rely in the possibility to reduce the maintenance and operational costs without losing in terms of system safety. These considerations led to the design of cost-effective solutions based on said technologies for the modernization of the regional low traffic lines that in Europe represent a big market slice [3]. The big challenge in the adoption of the GNSS technology for train localization is represented by the fulfillment of the safety integrity level (SIL 4) requirements defined by the Comité Européen de Normalization Électrotechnique (CENELEC). For this scope, the GNSS integrity concept has to be adapted to the rail context and relevant requirements have to be met.

The target is to achieve a tolerable hazard rate (THR) less than 10^{-9} hazard/(h × train), the same total hazardous failure rate of the traditional solution based on mechanical odometers and transponders deployed along the tracks at georeferenced points, named balises, [1], [5]–[7], [27], [38].

An important issue concerns signal in space (SIS) integrity assessment. A train location computed on the basis of measures either affected by satellite faults or strongly prejudiced by anomalous atmospheric propagation or local effects like multipath can lead to a misleading information (MI).

A MI happens when the magnitude of the position error exceeds the confidence interval associated to the nominal THR, computed by the receiver, and addressed as protection level (PL) in avionics, without a timely warning. Therefore, the use of an augmentation and integrity monitoring network (AIMN), able to detect and to notify to the on-board units (OBUs) the presence of hazards, is needed. For the aviation sector, wide area augmentation network (WAAN) and local augmentation network (LAN) systems have been developed. Satellite-based augmentation systems (SBAS) belong to WAAN, while ground-based augmentation systems (GBAS) to LAN class. Through the transmission of pseudorange measurements corrections and integrity monitoring (IM) messages, a high level of integrity can be achieved by the rover receiver. While through SBAS it is possible to achieve a THR in the order of 10^{-7} hazard/operation at regional/global level, GBAS is able to meet THR in the order of 10^{-9} hazard/operation (CAT-II and CAT-III or LAAS GSL D-F integrity requirements [18]).

In the literature, the IM algorithms have been studied for both cases: Receiver autonomous integrity monitoring (RAIM) [10], [11]–[13] and wide/local area (LA) integrity

monitoring network (IMN) [9], [14]–[17]. In this paper, we will focus on IMN.

Current SBAS systems, like WAAS (USA) and EGNOS (Europe), provide augmentation data that allow to reach meter accuracy. Moreover, they monitor only a single frequency of the GPS constellation. Thus, to reach the submeter accuracy required by train control system configurations that rely on GNSS also for determining on which track the train is operating (track discrimination), augmentation networks with a denser set of reference stations (RS) distributed on the area to be covered should be deployed [40]. In order to meet both accuracy and integrity requirements and reduce both capital and operational expenditure, several innovative architectures have been proposed [8], [9]. In particular, two-tiers architecture has been introduced in [17]. It is based on the joint use of an existing SBAS and an AIMN making use of low cost commercial off-the-shelf (COTS) RS.

Through the integration of the ranging and integrity monitoring stations (RIMS) of the first tier, constituted by the SBAS, and the RS of the second tier, it is possible to monitor, in a cost effective way, the integrity of both the SIS and the monitoring network itself, while computing the augmentation data. The dense network of the second layer allows to pave the way for high integrity network real-time kinematics (NRTK) implementations. Furthermore, as in the NRTK case, a hot backup procedure can be guaranteed in case of single reference layer.

Starting from the theoretical approach carried out in previous work [17], a real augmentation network implementing the two-tiers architecture has been deployed on the Sardinian railway testbed of RFI (the Italian Railway Infrastructure manager) and a test campaign carried out. To monitor integrity, this system implements a fault detection and exclusion (FDE) algorithm which is based on following.

1) SIS FDE, based on the monitoring of single difference residuals among satellites.
2) RS fault detection (FD), based on the monitoring of double difference (DD) residuals between stations of the first and the second tiers.

The relevant real-time IM system module, named local integrity function (LIF) has been implemented into GRD-Net, an existing Italian LAN that, before integration of LIF, provided augmentation without integrity.

LIF is in charge of implementing satellite, constellation, and RS IM based on the two-tiers algorithm.

A performance analysis has been carried out in real rail operative scenarios. IM tests have been performed through real GPS fault cases studied in the literature and injected on real GNSS raw measurement logged by the RS of the monitoring network, and a receiver on a train during its rides along the Cagliari–San Gavino railway of the testbed.

The performance analysis has been based on LIF functional, assembling, and integration tests on the field.

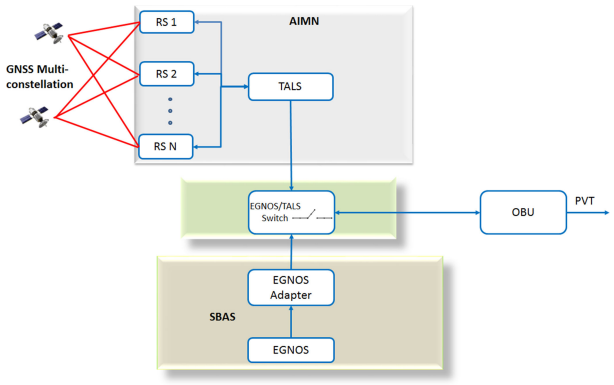

Fig. 1. Augmentation system architecture SBAS-LAN comparison.

Raw data and injected faults have been fed into a performance analysis tool (VIRGILIO) [31], able to assess the IM performance with respect to the target THR.

The tool generates the Stanford plot (e.g., [20]) and relevant availability, misleading, and hazardous misleading statistics.

Input data for the functional test, containing relevant SIS fault cases scenarios, have been generated in two ways.

1) *Real GNSS fault cases:* They have been selected from GPS NANU and Galileo GSA fault records; receiver independent exchange format (RINEX) files for the relevant time interval of the analysis have been used for this scope.
2) *Simulated fault cases:* Real GNSS measurements logged on the train have been edited for injecting ephemeris and clock errors; ramp models for pseudorange errors have been also used for sensitivity analysis.

In this paper, we report the assessment procedure and its results. In the assessment, a target THR $= 10^{-9}$ hazard/(h $\times$ train) has been adopted. The results have shown that the application of the new IM method is able to detect fault cases, exclude relevant faulty satellites in an efficient way, and to avoid MI. This paper is organized as follows. In Section II, an overview of local augmentation techniques used for IM purposes is reported. In Section III, the innovative IM algorithm is introduced. Section IV describes the adopted approach for the performance analysis and relevant test-bed architecture. Section V reports main conclusions of this study.

II. AUGMENTATION NETWORK ARCHITECTURES

In this section, we describe the main augmentation network architectures that have been proposed for the needs of train control systems. According to the literature, an augmentation system can operate on a small, local, region, or on a wider geographical area. The so-called LA AIMN belongs to the first case [33], [34], while the SBAS belong to the WAANs [35]. A comparison of the performance that can be expected from the use of EGNOS and from the use of an AIMN based on low-cost COTS receivers, for train positioning system can be found in [8]. As shown in Fig. 1,

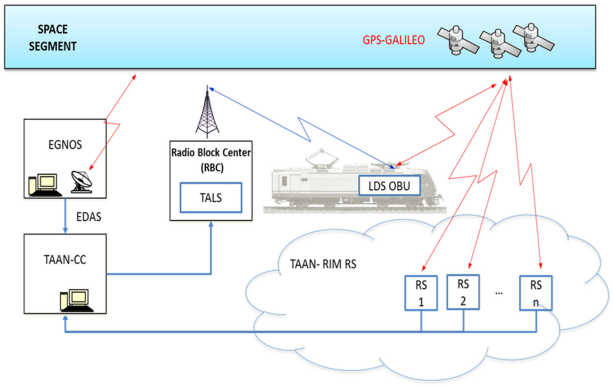

Fig. 2. Two-tiers augmentation network architecture.

where the configuration adopted for the comparison is reported, each train of the fleet is equipped with an OBU that receives data from the AIMN composed of a set of RS and from a track area location server (TALS) that collects data from the RS, processes them, and produces the LA integrity and augmentation data for the OBU.

The main difference between the local and wide area networks is in the FD capability. It is widely known how the LAN better mitigates the local effects like the atmospheric incremental delays, while the WAAN, thanks to the wider footprint, better compensates the global effects as the satellite ephemeris errors and clock offsets [17]. Starting by these two architectures, in [9], Neri *et al.* defined a new system that we will refer to as "two-tiers" augmentation network.

Between the major benefit of such an approach, we can list: 1) the possibility to implement the second tier, whose aim is to provide a denser set of observations, by means of low cost RS, whose health is monitored by comparing their observations with those of the first tier; 2) the possibility to detect both SIS faults and RS failures mitigating the threats arisen by the monitoring network malfunctioning, in order to be compliant with the railway accuracy and integrity requirements; and 3) the possibility to provide an IM also for constellations not monitored by the first tier.

Fig. 2 shows the two-tiers functional architecture.

In this scheme, the task of the track area augmentation network computing center (TAAN-CC) is to compute the augmentation data, containing IM information, then format and send them to the OBU. Relevant messages contain the following.

1) Estimated probabilities of fault of constellations and satellites.
2) Estimated pseudorange measurements variances.
3) Constellation and satellite health masks.

Such messages have been proposed within the ERSAT project, following a radio technical commission for maritime services (RTCM) like format (see [23]). Such format proposal has also been presented to a RTCM SC-104 plenary meeting, within the framework of the "IM for high precision applications" working group (see [22]). The algorithm implemented in the TAAN-CC for the assessment of the SIS healthiness has been reported in [17]. It can be employed for both single tier and two-tiers architectures.

III. SIS INTEGRITY ASSESSMENT

The ability to identify, and then to exclude, a measure affected by hazards (like satellite faults, strong multipath, ionosphere issues, etc.) is a key point in satellite-based train control system. This is due to the stringent safety requirements imposed CENELEC in terms of THR. In the literature, several approaches have been studied. We can distinguish between RAIM techniques and AIMN approaches. While RAIM involves the OBU receiver alone [10]–[13], the AIMN approaches rely on a network of RS deployed in known position. It has to be highlighted that the safety integrity has to be guaranteed at system level. Therefore, faults of the augmentation network itself have to be properly accounted for into the IM system. On the other hand, very demanding train operational phases (e.g., start of mission and protection of vital points) require a level of accuracy of 1 m or less with the same level of integrity. Moreover, train controls systems adopting adaptive modulation of train separation, like ERTMS level 3, require also discrimination among parallel tracks, whose interaxis is about 4 m. To achieve this goal, a decimeter accuracy is then required.

GBAS and SBAS accuracy and integrity have already been summarized in Section I. Concerning high-accuracy commercial systems, NRTK approach allows achieving centimeters level accuracy through quite dense RS networks (e.g., with interdistances of 70 km). Such systems make use of carrier phase GNSS measurements, needing the fixing of the integer of ambiguities through real-time kinematics (RTK) methods. Such networks are usually implemented for surveying applications, where integrity is not a tighter requirement. Therefore, IM systems are generally not implemented for RTK augmentation networks and user receiver relies to SBAS for SIS Integrity.

Innovative high-accuracy systems, as precise point positioning (PPP), have been developed based on wide area sparse RS monitoring systems and broadcasting of global corrections to the user. IM algorithms have been simulated and (e.g., carrier phase receiver autonomous IM) are currently a starting point for providing a high accuracy and integrity system. Time for convergence to 10-cm level [without considering PPP ambiguity resolution (AR) algorithms, still under consolidation] is today in the order of tenths of minutes.

In general, since the RS locations are known, SIS integrity can be evaluated by analyzing the deviation of the expected and observed RS pseudoranges. Some examples of such technique can be found in [14]–[17]. Obviously, a malfunctioning in the monitoring receiver can produce a misleading integrity assessment due to either false alarms (sometime referred as false exclusion), or miss detection. From this consideration, the necessity of RS integrity assessment arises.

In this paper, we will consider that the information on the first-tier RS healthiness provided by the first tier interface is fully reliable. In the following, the basic elements of the implemented IM system are summarized for the pseudorange measurements case, described in detail in Section III-C. It has to be highlighted that the proposed approach can be applied also to carrier phase measurements, once AR is performed or time-difference approach used. Details on the method that can be used to identify, and eventually to exclude from the network, monitoring receivers affected by failures can be found in [10].

A. Pseudorange Residual Definition

We refer to pseudorange residual (PR) for the *i*th satellite measured by the *n*th RS at the *k*th epoch as the quantity

$$\begin{aligned}\zeta_n^i[k] &= \rho_n^i[k] - \hat{r}_n^i[k] + c\delta\hat{t}_i^{\text{sat}}[k] - c\delta\hat{t}_n^{clk}[k] \\ &\quad - c\Delta\hat{\tau}_{i,n}^{\text{ion}}[k] - c\Delta\hat{\tau}_{i,n}^{\text{trop}}[k] \end{aligned} \tag{1}$$

where

- $\rho_n^i[k]$ measured pseudorange for the *i*th satellite by the *n*th RS at the *k*th epoch;
- $\hat{r}_n^i[k]$ estimated geometric distance between the *i*th satellite and the *n*th RS at the *k*th epoch estimated by means of the navigation message and the known receiver position;
- $c\delta\hat{t}_i^{\text{sat}}[k]$ estimated clock offset of the *i*th satellite at the *k*th epoch by using the navigation message;
- $c\Delta\hat{\tau}_{i,n}^{\text{ion}}[k]$ estimated ionospheric delay on the line of sight between the *i*th satellite and the *n*th RS at the *k*th epoch estimated by means of the Klobuchar model;
- $c\Delta\hat{\tau}_{i,n}^{\text{trop}}[k]$ estimated tropospheric delay on the line of sight between the *i*th satellite and the *n*th RS at the *k*th epoch estimated by means of the tropospheric model;
- $c\delta\hat{t}_n^{clk}[k]$ estimated clock offset of the *n*th RS at the *k*th epoch by using the least square (LS) estimator.

In case of multiconstellation processing, we should consider the interconstellation biases due to the different time offset between the constellations. For sake of compactness, we consider these terms as estimated and compensated, neglecting them in the following. If we consider the H_0 hypothesis (the satellite is healthy), the PR $\zeta_n^i[k]$ can be modeled as a Gaussian zero mean random variable with standard deviation σ_n^i. In the H_1 hypothesis (the satellite is affected by a fault), $\zeta_n^i[k]$ is still Gaussian distributed, but the mean is $\mu_n^i(\beta)$ where β models a wrong satellite position offset. In case of fault of different sources, β will represent an effective satellite position error that would have produced an error on the estimated receiver position of equal entity. PR is a widely used indicator to monitor ephemeris and satellite faults. In [14], Matsumoto *et al.* defined an approach to monitor satellite ephemeris errors, while in [15], Blanch *et al.* used a LS residual approach to identify and exclude multiple satellite faults.

B. Pseudorange *L2* Norm Square

In [16], Palma *et al.* defined a procedure to identify and exclude faulty satellite by jointly processing PRs coming from several RS deployed trackside. Let $y^i[k]$ be defined as

$$y^i[k] = \sum_{n=1}^{N_{\text{RS}}} \frac{\left(\zeta_n^i[k]\right)^T \zeta_n^i[k]}{\left(\sigma_n^i\right)^2} \tag{2}$$

where σ_n^i is the standard deviation of ζ_n^i, and $y^i[k]$ can be considered as the weighted *L2* norm square of the vector $\underline{\zeta}^i[k]$ defined as

$$\underline{\zeta}^i[k] = \left[\zeta_1^i[k]\ \zeta_2^i[k] \cdots \zeta_{N_{\text{RS}}}^i[k]\right]^T \tag{3}$$

where

$$\zeta_n^i(k) = \begin{bmatrix} \zeta_n^{i,1}(k) \\ \vdots \\ \zeta_n^{i,i-1}(k) \\ \zeta_n^{i,i+1}(k) \\ \vdots \\ \zeta_n^{i,N_{Sat}}(k) \end{bmatrix} \tag{4}$$

is the vector of single difference residuals for the *n*th RS and *i*th satellite, and $y^i[k]$ in the H_0 hypothesis follows a centered chi-square distribution with $N_{\text{RS}} - 1$ degrees of freedom, while it follows in the H_1 hypothesis, a noncentered chi-square distribution with $N_{\text{RS}} - 1$ degrees of freedom and a parameter of noncentrality $\lambda(\beta)$. For the standard deviations σ_n^i, a classical elevation dependent model can be adopted. As an alternative, values computed by the network control center (CC) filter can be employed (e.g., when an NRTK solution is developed in parallel). Here, an elevation model, based on classical SBAS modeling, has been used.

According to Neyman–Pearson criterion, the *i*th satellite is excluded if $y^i[k]$ exceeds the exclusion threshold γ whose value can be set as

$$\gamma = D^{-1}_{\chi^2_{N_{\text{RS}}-1}}\left(1 - P_{fa}\right) \tag{5}$$

where $D^{-1}_{\chi^2_{N_{\text{RS}}-1}}$ is the chi-square inverse cumulative distribution with $N_{\text{RS}} - 1$ degrees of freedom, and P_{fa} is the imposed false alarm probability.

For the aviation case (e.g., [26]), typical P_{fa} values are 10^{-3} and 10^{-4}. Therefore, the value of 10^{-3} has been allocated for the performance analysis carried out in this study. For a given P_{fa}, the exclusion threshold can be derived through numerical inversion of the generalized chi square (e.g., [29]).

Consequently, the miss detection probability P_{md} will be

$$P_{md} = D^{nc}_{\chi^2_{N_{\text{RS}}-1}}(\gamma, \lambda) \tag{6}$$

where $D^{nc}_{\chi^2_{N_{RS}-1}}$ is the chi-square inverse cumulative distribution with $N_{\text{RS}} - 1$ degrees of freedom.

More in detail, the exclusion process follows the following criterion: the $y^i[k]$ indicator is evaluated for each satellite belonging to the healthy list (initially, we suppose that all the satellites are healthy), and the largest value is selected. Then, if the largest $y^i[k]$ exceeds the threshold γ, the corresponding satellite is labeled as faulty and excluded. Then, the set $\{y^i[k]\}$ is refreshed considering the updated list of healthy satellites, and the algorithm is repeated until the largest $y^i[k]$ is below the threshold, or all the visible satellites have been excluded.

C. Pseudorange DD *L*2 Norm Square

In [9], Neri *et al.* proposed a multiple FD algorithm based on DD residual. The algorithm proposed has been designed to identify and exclude faulty RS. Here, it is extended to identify and exclude faulty satellites.

Let consider the satellites *i*th and *j*th observed by the *m*th and *n*th RS. The DD PR at the *k*th between the entities can be defined as

$$\zeta_{m,n}^{i,j}[k] = \zeta_m^i[k] - \zeta_m^j[k] - \zeta_n^i[k] + \zeta_n^j[k]. \tag{7}$$

Let define the DD residual vector as

$$\underline{\xi}_{m,n}^{i}[k] = \left(\zeta_{m,n}^{i,1}[k]\ \zeta_{m,n}^{i,2}[k] \cdots\ \zeta_{m,n}^{i,N_{\mathrm{SAT}}}[k]\right)^T. \tag{8}$$

Let the satellite fault indicator $z^i[k]$ be

$$z^i[k] = \sum_{m=1}^{N_{\mathrm{RS}}} \sum_{n=1}^{N_{\mathrm{RS}}} \left(\underline{\xi}_{m,n}^{i}[k]\right)^T \underline{\xi}_{m,n}^{i}[k] \tag{9}$$

$z^i[k]$ in the H_0 hypothesis follows a centered generalized chi-square distribution with $N_z = (N_{\mathrm{SAT}} - 1) \cdot (N_{\mathrm{RS}} - 1)^2$ degrees of freedom. According to the Neyman–Pearson criterion, the exclusion threshold γ can be set as

$$\gamma = D_{G\chi^2_{N_z}}^{-1}\left(\Lambda, 1 - P_{fa}\right) \tag{10}$$

where Λ_i are the eigenvalues of the covariance matrix of PR DDs, and $D_{G\chi^2_{N_z}}^{-1}(\cdot)$ is the centered generalized chi-square distribution

$$D_{G\chi^2_{N_z}} = \frac{1}{\prod_{i=2}^{N_z}\Lambda_i} D_{\chi^2_1}\left(\frac{x}{\Lambda_1}\right) * p_{\chi^2_1}\left(\frac{x}{\Lambda_2}\right) * \cdots * p_{\chi^2_1}\left(\frac{x}{\Lambda_{N_z}}\right). \tag{11}$$

In the H_1 hypothesis, the test statistics follow a noncentered generalized chi-square distribution with N_z degrees of freedom and a parameter of noncentrality $\mu(\beta)$. Then, the miss detection probability P_{md} will be

$$P_{md} = D_{G\chi^2_{N_z}}^{nc}(\gamma, \Lambda, \mu). \tag{12}$$

The exclusion approach follows the following criterion: the $z^i[k]$ indicator is evaluated for each satellite belonging to the healthy list (initially, we suppose that all the satellites are healthy). After that if the largest value of the indicator exceeds the exclusion threshold, the corresponding satellite is labeled as faulty and discarded. The algorithm is repeated until the largest value of the indicator is below the threshold, or all the satellites have been discarded. The algorithm workflow is depicted in the following pseudocode.

- Insert all visible satellites in the *HealthySat_List* (i.e., label each satellite as healthy)
- Set *DetectFaultySatellites* = TRUE
- *Repeat until* (HealthySat_List is not Empty AND *DetectFaultySatellites*}
  - *For each* satellite *i in HealthySat_List*
    - Compute the DD residual vector corresponding to the *HealthySat_List* $\underline{\xi}_{m,n}^{i}[k] = (\zeta_{m,n}^{i,1}[k]\ \zeta_{m,n}^{i,2}[k] \cdots\ \zeta_{m,n}^{i,N_{SAT}}[k])^T$
    - Compute $z^i[k] = \sum_{m=1}^{N_{\mathrm{RS}}} \sum_{n=1}^{N_{\mathrm{RS}}} (\underline{\xi}_{m,n}^{i}[k])^T \underline{\xi}_{m,n}^{i}[k]$
  - Select the index *i* corresponding to the largest $z^i[k]$ $\hat{i} = \mathrm{Arg}\left\{\underset{i}{\mathrm{Max}}\, z^i[k]\right\}$
  - *If* $z^{\hat{i}}[k] > \gamma$ *then*
    - Mark the satellite as faulty and remove it from the *HealthySat_List*
    - Recalculate γ
  - *else*
    - *DetectFaultySatellites = FALSE*
  - *End If*
- *End Repeat*

D. Literature Review Analysis

Considering the method presented in Section III-B, the main limitation is the dependence of the system by the receiver clock offset estimation. In fact, $\zeta_n^i[k]$ is affected by the error in the receiver clock offset estimation. This means that a faulty satellite can lead to an incomplete receiver clock compensation corrupting all the residuals generated by that RS. This limitation has been removed in the algorithm proposed in Section III-C.

In fact, working with the DD, all the clock offset components will be canceled out. On the other side of the coin, we have the impossibility to detect and exclude satellite faults due to satellite clock. The other advantage of using Section III-C approach instead of the one in Section III-B is the possibility to reveal more efficiently the presence of multiple satellite faults.

The main limitation of the Section III-C approach is represented by the computational cost in the evaluation of the exclusion threshold.

The presented approach offers an advantage in robustness with respect to classical standalone systems (e.g., SBAS or GBAS), due to the fact that different systems are integrated. In such a way, the impact of common-mode errors is reduced.

This is evident in the case of RS multiple failure. The integration of external, certified SBAS RIMS for performing DDs allows to avoid possible cancellation of common-mode errors, and a more robust RS detection and exclusion.

Concerning the total constellation fault monitoring, consistent errors are detected through the following test statistics:

$$z_{\varepsilon_P^c} = \left(\varepsilon_P^c(k)\right)^T \mathbf{R}_{\varepsilon_P^c}^{-1} \left(\varepsilon_P^c(k)\right) \tag{13}$$

where $\mathbf{R}_{\varepsilon_{P_n}^c}$ is the covariance matrix of the position error of the nth RIMS.

E. Advantages of the New Approach

The proposed two-tiers algorithm leads to several advantages with respect to classical LA systems that are needed for achieving THR for train position determination function in the order of 10^{-9} hazard/h per train.

Traditional LA systems (e.g., GBAS or International Association of Marine Aids to Navigation and Lighthouse Authorities DGPS systems) are based on the installation of high grade and relevant cost RS with a tight level of certification (e.g., to be compliant to D0-229D for the aviation case). As a matter of example, the implementation of a GBAS RS network is in the order of 120 k€ for a classical four reference receivers configuration (see [40]). On the other hand, IM is typically used in some application fields, as maritime beacons, with very high-cost DGNSS RS implementation and maintenance.

Geodetic networks are based on geodetic COTS GNSS receiver. The price of a multiconstellation and multifrequency RS is currently in the order 10 k€ and is continuously decreasing. Typically, such RS networks are developing RTK and NRTK services, and are operative for supporting national mapping authorities for land administration. Relevant interdistances are in the order of 70 km. Such services are currently used for surveying purposes. On the other hand, maximum distance from the reference receiver allowed for GBAS is 23 nautical miles.

Therefore, a cost saving of at least 15 k€ per reference receiver is foreseen with respect to a GBAS, leading to a total saving of at least 60 k€, with a greater service coverage area.

The new algorithm, presented in this study, allows reducing such costs through the integration of global (e.g., SBAS RIMS) and local solutions (COTS reference receivers).

A two-tiers CC can integrate its own second layer network based on COTS and, possibly, implement a densification through external RS. Concerning the first layer, it is assumed that data coming from SBAS, certified RIMS, are provided for free by relevant institutions [e.g., EGNOS data access service (EDAS)].

Therefore, it is evident how the possibility to use COTS receivers for implementing the needed GNSS high accuracy and integrity services leads to a cost saving of at least one order of magnitude.

The disadvantage is that such solution depends on the availability of first-layer GNSS raw data for free. Just in case, such access is not available or relevant fees have to be paid for getting them, proper agreements have to be setup between SBAS stakeholders and national operators.

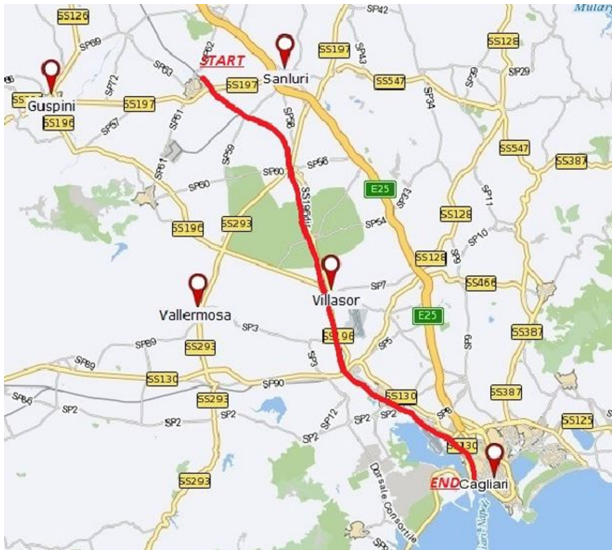

Fig. 3. Two-tiers algorithm testbed.

However, such services generate evident public benefits, and it is expected that national authorities (e.g., ministries of transport) can favorite their implementations.

IV. PERFORMANCE ANALYSIS

A performance analysis testbed has been implemented through the integration of the two-tiers algorithm into an existing GNSS network CC, an on-board COTS receiver on a train, and a rail performance analysis tool.

In order to test the two-tiers algorithm performances, several fault scenarios (for satellite, constellations, and RS) have been defined. Faults are generated using as input raw data RINEX files from existing historical GPS faults or through recorded RS and OBU files editing.

The performance analysis tool is able to take as input RS and OBU files and generate relevant integrity and accuracy performances statistics for the rail application since railway requirements have been set up into the software (e.g., THR for deriving the correct PL).

Probability of faults for satellite, constellations, and RS, needed for the two-tiers algorithm implementation has been derived from literature or GNSS network operations statistics.

The output of the performance analysis is the Stanford plot for a simulated or real train track, subject to GNSS or local augmentation fault. A comparison of performances with or without the 2-tiers algorithm adoption has been analyzed.

A test bed, developed within the EU Horizon 2020 Project named ERSAT-EAV [36], has been used at this scope. The test site is shown in Fig. 3, where the red line indicates the Cagliari-S. Gavino railway where the real-time tests have been carried out and the location of the RS for implementing the two-tiers based augmentation network are reported.

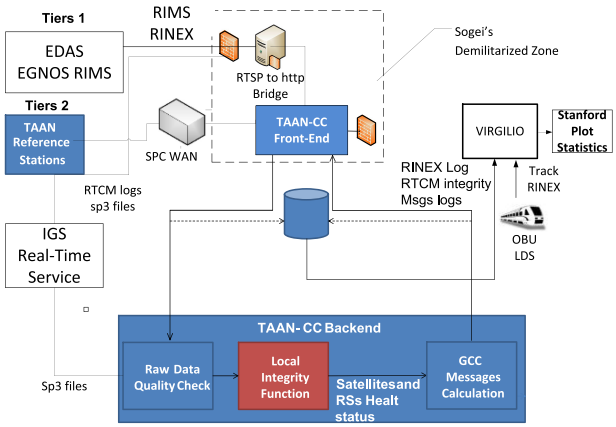

Fig. 4. Performance analysis architecture.

A. Performance Analysis Architecture

Relevant test architecture is reported in Fig. 4. The track area augmentation network (TAAN) includes five multiconstellation and multifrequency COTS receivers installed on public administration sites. They are connected to a high-precision operating network named GRDNet (GNSS R&D network) located in Rome. A high QoS communication network is used at this scope. All the interfaces are using standard connection protocol and data format (RTCM 3 messages and networked transport of RTCM via IP). The two-tiers algorithm has been implemented within the GRDNet CC, and it works in real time. New RTCM messages have been defined for the communication of relevant integrity parameters to the TALS. The connection to the EGNOS RIMS (constituting the first tier) has been carried out through the EDAS.

A LIF software module has been created and integrated into the CC for implementing the two-tiers algorithm. It is in charge of performing GPS and GALILEO constellations, as well as RS FDE through the two-tiers algorithm described in Sections III-B, III-C, and III-D. Relevant results are used by the message formatter for deriving IM parameters to be sent to the user. Precise ephemeris and clock are gathered in real time from the IGS-RTS (international GNSS service real time).

B. Performance Test Methodology and Assumptions

The functional test methodology is the following. An IM performance analysis tool, named VIRGILIO [31] and used in previous ESA and GSA projects for performance analysis on rail, has been configured with the SIL 4 safety requirements.

The tool takes as input GNSS raw measurements in RINEX format and the georeferenced railway database (ordered set of the geographic coordinates of the polyline approximating each track), and generates the Stanford plot (e.g., [20]) and relevant availability, misleading, and hazardous misleading statistics.

Input data for the functional test, containing relevant SIS fault cases scenarios, are generated in two ways.

TABLE I
Functional Test Phases

TAAN RSs Tests	RSs configuration and interfacing tests
General TAAN-CC Tests	Network CC is tested while interfacing with GNSS RIMS and RSs.
LIF System Test	2-tiers algorithm is tested through real GNSS fault cases injection (probability of fault generation (single satellite, constellation, RSs) or integrity fault generation in real time (RTCM upgraded messages).
TAAN Integration Test	The augmentation system performances, based on the 2-tiers algorithm, are tested through four scenarios, based both on real GNSS and injected fault cases that have been carried out in real time (RTCM upgraded messages). TAAN-CC injects faults in the raw measurements, while the augmentation system detects them. Relevant satellites have been excluded from the messages sent to the user; satellite fault is recognized by the OBU, and not applied to the train positioning solution.

1) *Real GNSS fault cases:* A relevant set of real fault cases has been selected from GPS NANU [21] and Galileo GSA fault [20] records; RINEX files for the same time interval (therefore containing the declared fault) have been used as sources.
2) *Simulated fault cases:* Real GNSS measurements, acquired by a receiver on the train during daily rides, have been injected with relevant SIS faults that have been generated through models described in the literature.

The possibility to use both kinds of inputs allows a great testing flexibility and covering all the major fault cases. Furthermore, while real GNSS faulted data allow testing the algorithm in an operative case, simulated data allow performing sensitivity analysis on single parameters, and opportunely set thresholds and fault injection windows. The functional tests have been organized in four groups.

1) TAAN RS tests.
2) General TAAN-CC tests.
3) LIF system tests.
4) TAAN integration tests.

Tests have been performed both in postprocessing and real time. For the real-time case, faults have been added by the TAAN-CC to relevant raw measurements gathered by RS. The LIF is, therefore, able to analyze the faulted value, detect the relevant, and send the relevant integrity messages to the OBU on the train. In Table I, the functional test phases are reported.

For the two-tiers algorithm functional test, RINEX files corresponding to some literature fault cases have been analyzed in order to evaluate the FD capability.

1) *LIF Integration Test:* The following tests have been performed.

1) *Real cases clock anomaly tests:* Satellite exclusion using two-tiers algorithm applied on RINEX files containing the recorded fault period.

2) *Simulated pseudorange error:* A ramp error on a 30-min time window is added to a pseudorange measurement of a satellite; clock error has been simulated through ramp

$$\Delta\rho^{i}_{PR}(t) = d^{i}(t - t_0) \tag{14}$$

where d^i is the pseudorange error drift (set to 0.1 m/s, [41]), t_0 is the starting time for the clock anomaly, and t is the current measurement time.

3) Clock anomaly simulated for a satellite through RINEX navigation file editing.

For each test, data are processed with and without the LIF 2-tiers algorithm activation to verify the FD performances.

Concerning the fault probabilities, relevant values are derived from historical GNSS fault cases.

As a matter of example, classical probability of fault satellite for an early satellite constellation can be in the order of 1 h per year, leading to a P_{sat} of 10^{-4}.

1) P_{const} *(probability of constellation fault):* 10^{-4} and 10^{-8} [25]; the first one is intended for a value relevant for a still not completely operational constellation (e.g., GALILEO), while the second is applicable for a mature constellation, like the current GPS.
2) P_{sat} *(probability of satellite fault):* 10^{-5} [26].
3) P_{RS} *(probability of RS fault):* 10^{-5} ([18] and GRDNet statistics).
4) P_{FA}*:* 10^{-3}, following classical aviation assumption [26].

In next evolutions, it is foreseen to introduce a real-time estimation of relevant probabilities of fault in LIF software.

The details of the clock anomaly test due to real fault cases are here reported.

1) Test 1—Date/time 2006 Jul 31 22:15, PRN 03, clock anomaly.
2) Test 2—Date/time 2006 Aug 25 12:30, PRN 29, clock anomaly.
3) Test 3—Date/time 2009 Jun 26 09:30, PRN 25, clock anomaly.
4) Test 4—Date/time 2012 Jun 17 00:10, PRN 19, clock anomaly.

All the faults have been detected correctly. As a matter of example, in Fig. 5, the result for test 2 is reported. As can be seen in Fig. 5(b), the single difference residuals with respect to GPS PRN 29 are increasing, and at about epoch 47 600, the exclusion threshold is overcome.

After that time, the satellite is declared as faulted, excluded by the calculation by the relevant residual difference plot. In the visibility plot Fig. 5(a), PRN 29 is correctly excluded after that epoch. A satellite fault has been also simulated.

As reported in Fig. 6, a ramp error has been injected on PRN 12, starting at 15, for 30 min.

The LIF is able to detect the anomaly and exclude the satellite [see Fig. 6(a)].

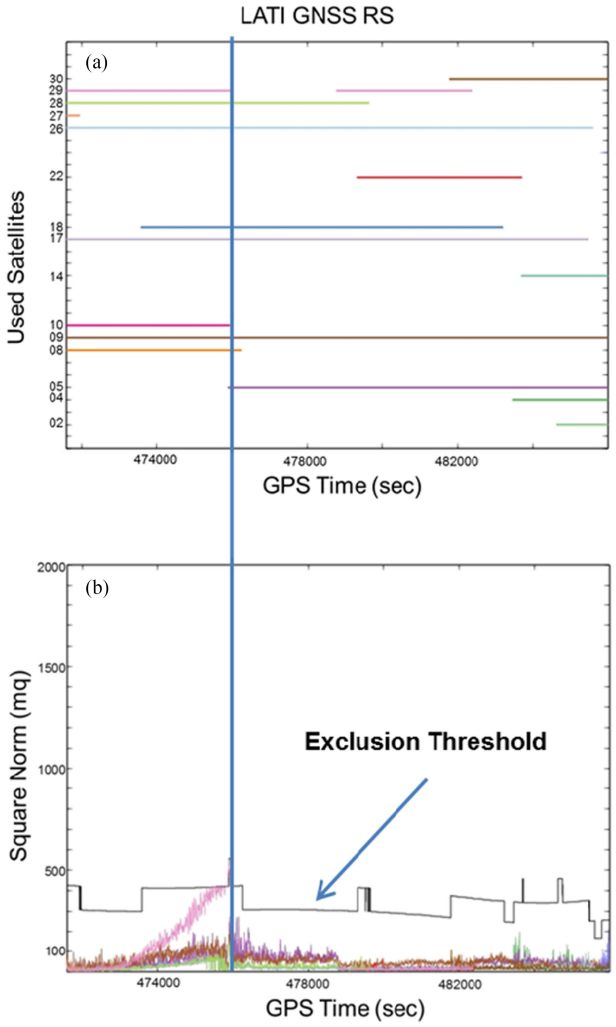

Fig. 5. LIF functional test (LATINA GNSS RS, 2006 August 25 GPS PRN29 clock anomaly); (a) used GPS satellites; (b) square norm of single difference residuals per satellite and exclusion threshold (black line).

2) *TAAN Integration Test:* For the TAAN integration test, three test scenarios have been defined.

The aim of the test is to develop the whole IM chain and to simulate relevant performance in a rail operational environment (without applying existing TCS monitoring). In order to analyze relevant performances, the results of the IM application have been compared with the reference case where the same fault happened, and no IM was applied.

Both rail ride simulation and real tests with a receiver on a train have been carried out. Faults have been injected, and LIF FDE algorithms have been applied in real time in the second case. Performance analysis has been carried out considering an alert limit of 30 m (this value has been set according to ERSAT-EAV project requirements [36]). The position estimations and the PLs are evaluated explicitly accounting for the *a-priori* knowledge of the track as it has been described in [1]. In this paper, for sake of compactness, the uncertain in the track database has been neglected. The following test scenarios, developed within the ERSAT-EAV project [36], [37], have been developed and are here described in detail.

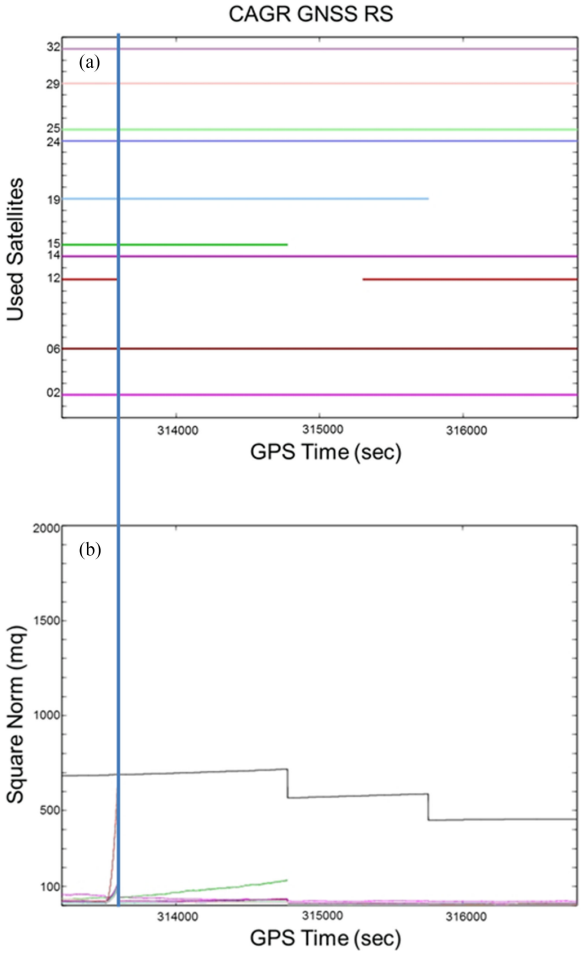

Fig. 6. LIF functional test (CAGR GNSS RS, 2016 APR 04 15:00 simulated ramp error on PRN 12 for 30 min); (a) used GPS satellites; (b) square norm of single difference residuals per satellite and exclusion threshold.

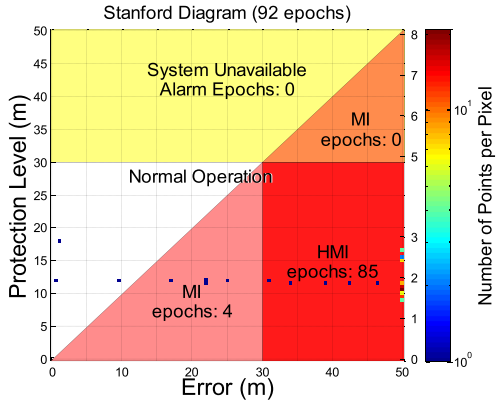

Fig. 7. Scenario 1 test case results (no LIF).

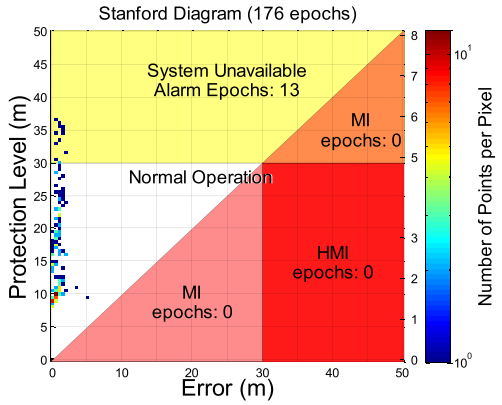

Fig. 8. Scenario 1 test case results (LIF applied).

Scenario 1–Static test: Two existing Sogei GRDNet RS (ROMA and RIETI) and a fixed RS located in Fiano (Italy), used as an OBU, located in the center of Italy on Day 17 June 2012 have been selected, when a fault on PRN 19, due to a clock anomaly occurred at 00:10. ROMA and RIETI RS have an interdistance of 60 km, and are about 50 km far from the Fiano receiver. The test is intended to perform a first integration test through static receivers for validating LIF performances.

Scenario 2–Simulated OBU: Two RS have been used in the area of the Sardinia testbed. Two TAAN RS (CAGR and VILL) and a simulated moving train over a synthetic track form Cagliari railway station to Località Produttiva (Villacidro) are considered. A fault on PRN 2 is simulated modifying a satellite clock offset bias on the RINEX navigation file day dated March 13 2016. CAGR to VILL interdistance is in the order of 24 km. The test is intended to perform a validation test LIF performances for a moving object.

Scenario 3–Real rail track: Two TAAN RS CAGR and SANL, installed in Cagliari and Sanluri, respectively, and a real test on a train moving in the track from San Gavino to Cagliari, are considered. The scenario is placed in Sardinia. Since we are working offline, the ground truth has been generated checking the absence of real GNSS faults in IGS and EDAS repository. A fault on PRN 12 is simulated, modeling an error as a ramp on the pseudorange, and inserted into the LIF monitoring process for real-time FDE. The test is intended to validate the LIF FDE performance in a real rail operative scenario. The test was carried out on day 2016 April 6. It has to be noted that the RS interdistances and the RS to rover receiver distance are within acceptable range both for pseudorange only and for network RTK operations (maximum of 70-km RS distance for the latter). In the present analysis, we are dealing with pseudorange measurement only.

For scenario 1, relevant results are reported in Figs. 7 and 8. On the first figure (no LIF), the performances without the application of the LIF algorithm are presented, while on the second (LIF), the LIF FDE one is applied, and PRN 19 satellite excluded. The MI situation is fully recovered by the application of the LIF. It has to be noted that in presence of faults, a preliminary check is performed by the performance analysis tool. Therefore, epochs with excessive square residuals are deleted and not taken into account into the total number of shown epochs. This is the reason why the number of epochs for the case where LIF is not applied is less than the ones with LIF applied.

In the scenario 2 plots, relevant OBU data, taking the Fiano RS as source, are calculated with a 30 s rate over a

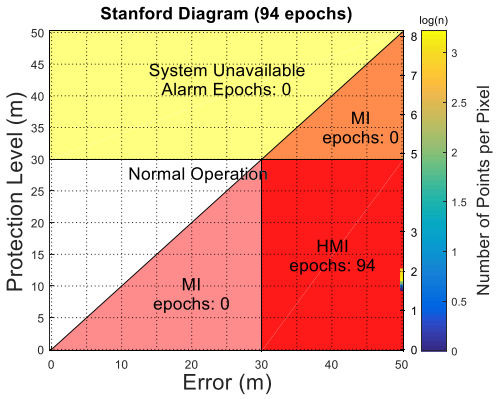

Fig. 9. Scenario 2 test case results (no LIF).

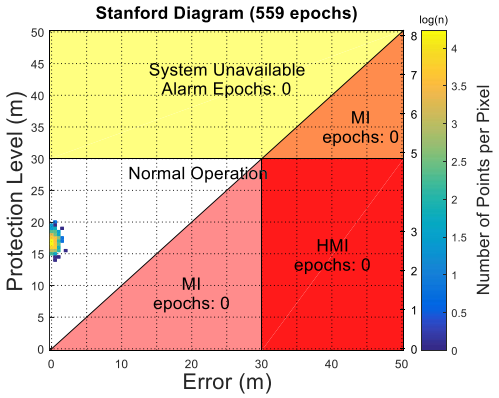

Fig. 10. Scenario 2 test case results (LIF applied).

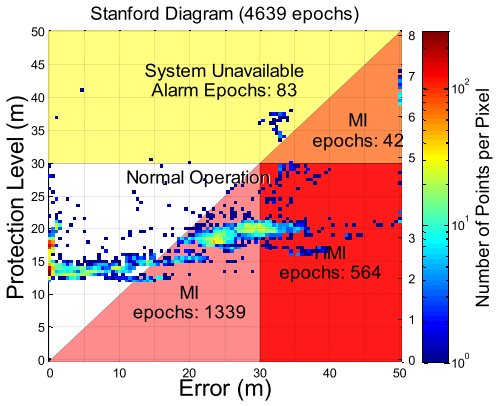

Fig. 11. Scenario 3 test case results (no LIF).

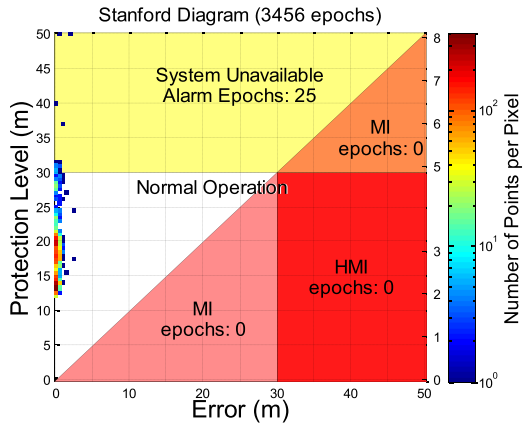

Fig. 12. Scenario 3 test case results (LIF applied).

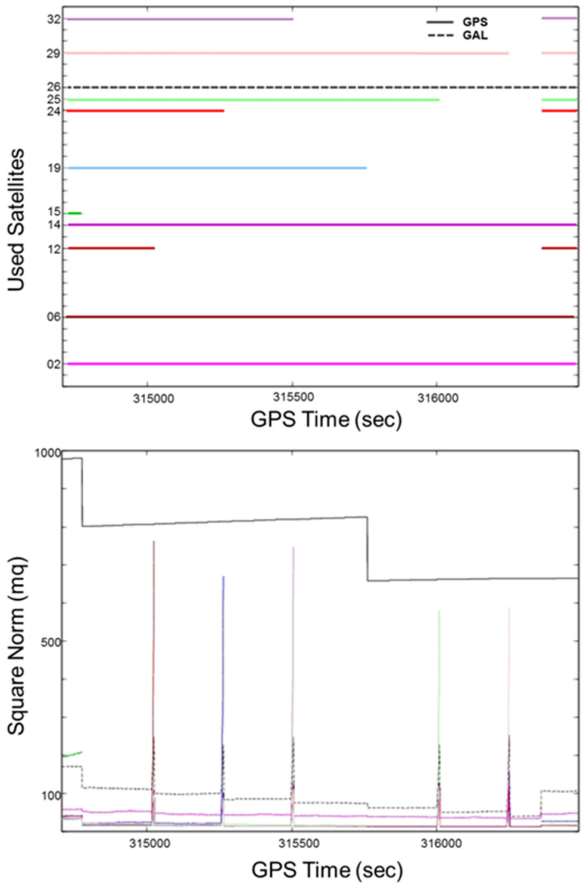

Fig. 13. Multiple SIS failure (LIF applied), SIS visibility (top), and detection plot (bottom).

period of about 5000 s. In this case, the number of epochs for the reference case is less than the relevant one in case of LIF FDE. This is due to the fact that, when a position cannot be calculated, the performance analysis excludes the relevant epoch from the total count. It has been demonstrated that the FDE algorithms allows promptly detecting the fault satellite and excluding it for the whole fault duration. Scenario 2 results are shown in Figs. 9 and 10. The extreme situation of full HMI case is fully recovered by the application of the LIF. Scenario 3 results are reported in Figs. 11 and 12. The simulated ramp error on the pseudorange (with relevant slope reported in Section IV-B1) introduces in this case relevant MI and HMI situations. After the application of the LIF two-tiers FDE, all the MI and HMI situations are covered.

A multiple satellite fault analysis has been carried out within the framework of the railway high integrity navigation overlay system Horizon 2020 project [30]–[32]. In this case, simulated errors are injected on pseudorange as ramps for multiple satellites. The data were collected on the OBU of the testbed train on 6 April 2016. Erroneous data are first introduced on PRN 12 and then on PRN 24, 32, 25, and 29. Relevant performances of the LIF algorithm are reported in Fig. 13. As can be seen in that figure, single

satellite faults are detected and excluded in case of multiple failures. The reported processing time for epoch-by-epoch two-tiers algorithm is in the order of 40 ms.

Concerning the communication losses and latency, a particular effort has been spent for minimizing it. High QoS links between single RS and the CC have been deployed. Relevant delays are monitored in real time. The maximum detected latency is in the order of 20 ms.

Processing delays for FD are 40 ms, derived from operative tests. Out of mobile communication link, a total maximum latency in the order of 100 ms can be expected. Furthermore, it has to be noted that excessive communication delays are managed by the TCS operational constraints (the PL varies accordingly), and the communication means in the railway sector are evolving.

V. CONCLUSION

The adoption of satellite localization for train control system is a challenge task due to the high-integrity requirement for rail operations. To this aim, an innovative method based on a two-tiers local augmentation and global monitoring networks has been developed. This architecture has been validated by detailed analyses using real data generated from fault cases described in literature and GNSS raw data acquired during rail operations. A local augmentation system able to implement in real time the proposed algorithm has been developed for this scope. The performance analysis results have shown that the new approach is able to detect and exclude faulted satellites meeting the rail safety requirements. At the same time, this architecture represents a cost efficient solution to be implemented, since it reuses existing augmentation networks instead of realizing high-integrity networks only for the rail applications.

ACKNOWLEDGMENT

The authors would like to thank G. Olivieri and F. Fritella from Sogei for their hard work on the LIF development and testing within the GRDNet network software.

REFERENCES

[1] A. Neri, A. Filip, F. Rispoli, and A. M. Vegni
An analytical evaluation for hazardous failure rate in a satellite-based train positioning system with reference to the ERTMS train control systems
In *Proc. 5th Int. Tech. Meet. Satellite Div. Inst. Navig.*, Nashville, TN, USA, 2012, pp. 2770–2784.

[2] ERTMS (European Rail Traffic Management System), Nov. 14, 2017. [Online]. Available: www.ec.europa.eu/transport/modes/rail/index

[3] ERTMS Levels, Different ERTMS/ETCS Application Levels to Match Customers' Needs, Factsheets, 2014.

[4] P. Salvatori, A. Neri, C. Stallo, and F. Rispoli
Ionospheric incremental delay models in railway applications
In *Proc. IEEE Metrology Aerosp. Conf.*, Jun. 4–5, 2015, pp. 251–255.

[5] A. Filip and F. Rispoli
SIL 4 compliant train location determination system based on dual-constellation EGNOS-R Interface for ERTMS/ETCS
In *Proc. Int. Symp. Certification GNSS Syst. Serv.*, Dresden, Germany, Jul. 8–9, 2014, pp. 109–114.

[6] A. Filip and F. Rispoli
Safety concept of GNSS based train location determination system SIL 4 compliant for ERTMS/ETCS
In *Proc. Eur. Navig. Conf. GNSS*, Rotterdam, The Netherlands, 2014, p. 15.

[7] A. Filip, J. Beugin, and J. Marais
Safety concept of railway signaling based on Galileo safety-of-life service
In *Proc. 11th Int. Conf. Comput. Syst. Des. Oper. Railway Other Transit Syst.*, Toledo, Spain, Sep. 15–17, 2008, pp. 103–112.

[8] P. Salvatori, A. Neri, C. Stallo, V. Palma, A. Coluccia, and F. Rispoli
Augmentation and integrity monitoring network and EGNOS performance comparison for train positioning
In *Proc. 22nd Eur. Signal Process. Conf.*, Sep. 1–5, 2014, pp. 186–190.

[9] A. Neri, R. Capua, and P. Salvatori
High integrity 2-tiers augmentation systems for train control systems
In *Proc. ION Pac. PNT Meet.*, Apr. 20–23, 2015, pp. 434–453.

[10] B. Muhammad, E. Cianca, and A. M. Salonico
Multi GNSS advanced RAIM: An availability analysis
In *Proc. IEEE Metrology Aerosp. Conf.*, May 29–30, 2014, pp. 28–33.

[11] M. Joerger and B. Pervan
Solution separation and chi-squared ARAIM for fault detection and exclusion
In *Proc. IEEE/ION Position, Location Navig. Symp.*, May 5–8, 2014, pp. 294–307.

[12] J. Blanch, T. Walter, P. Enge, and V. Kropp
A simple position estimator that improves advanced RAIM performance
IEEE Trans. Aerosp. Electron. Syst., vol. 51, no. 3, pp. 2485–2489, Jul. 2015.

[13] J. Blanch, T. Walter, and P. Enge
Satellite navigation for aviation in 2025
Proc. IEEE, vol. 100, no. Special Centennial Issue, pp. 1821–1830, May 13, 2012.

[14] S. Matsumoto, S. Pullen, M. Rotkowitz, and B. Pervan
GPS ephemeris verification for local area augmentation system (LAAS) ground stations
In *Proc. Inst. Navig. GNSS Conf. GPS*, Nashville, TN, USA, Sep. 14–17, 2009, pp. 691–704.

[15] J. Blanch, T. Walter, and P. Enge
Fast multiple fault exclusion with a large number of measurements
In *Proc. Inst. Navig. Int. Tech. Meet.*, Dana Point, CA, USA, 2015, pp. 696–701.

[16] V. Palma, P. Salvatori, C. Stallo, A. Coluccia, A. Neri, and F. Rispoli
Performance evaluation in terms of accuracy positioning of local augmentation and integrity monitoring network for railway sector
In *Proc. IEEE Metrology Aerosp. Conf.*, May 29–30, 2014, pp. 394–398.

[17] P. Salvatori, A. Neri, C. Stallo, and F. Rispoli
A multiple satellite fault detection approach for railway environment,
In *Proc. 15th Int. Conf. ITS Telecommun.*, Warsaw, Poland, 2017, pp. 1–5.

[18] Minimum Aviation System Performance Standards for the Local Area Augmentation System (LAAS), RTCA DO-245A, 2004.

[19] 2011. [Online]. Available: http://www.navipedia.net/index.php/Integrity

[20] Oct. 2018. [Online]. Available: https://www.gsc-europa.eu/system-status/Constellation-Information

[21] Oct. 2018. [Online]. Available: https://www.navcen.uscg.gov/?pageName=gpsAlmanacs

[22] R. Capua
High precision integrity monitoring WG-work update status
In *Proc. Radio Tech. Commission Maritime Serv. RTCM Plenary Meet.*, Jan. 28, 2016, p. 33.

[23] D4.5 -TAAN Sub-System Document, ERSAT EAV ERSAT-EAV-S-0-000-02Internal Document, 2016.

[24] T. Murphy, C. Shively, L. Azonlai, and M. Brenner
Fault Modeling for GBAS Airworthiness Assessments, MITRE Corporation, Bedford, MA, USA, 2012.

[25] J. Blanch *et al.*
Advanced RAIM user algorithm description: Integrity support message processing, fault detection, exclusion, and protection level calculation
In *Proc. 25th Int. Tech. Meet. Satellite Div. Inst. Navig.*, 2012, pp. 2828–2849.

[26] T. Walter and J. Blanch
Airborne mitigation of constellation wide faults
In *Proc. Int. Tech. Meet. Inst. Navigation*, Jan. 26–28, 2015, pp. 676–686.

[27] ETCS Application Levels 1 & 2—Safety Analysis, SUBSET-088, UNISIG, 2008.

[28] *Minimum Operational Performance Standards for Global Positioning System Airborne Equipment*, RTCA DO-229, 2009.

[29] P. Duchesne and P. Lafaye de Micheaux
Computing the distribution of quadratic forms: Further comparisons between the Liu-Tang-Zhang approximation and exact methods
Comput. Stat. Data Anal., vol. 54, pp. 858–862, 2010.

[30] L. S. Lo *et al.*
Projected performance of a baseline high integrity GNSS railway architecture under nominal and faulted condition
In *Proc. 30th Int. Tech. Meet. Satellite Div. Inst. Navig.*, Portland, OR, USA, Sep. 25–29, 2017, pp. 2148–2171.

[31] C. Stallo *et al.*
GNSS-based location determination system architecture for railway performance assessment in presence of local effects
In *Proc. IEEE ION Position, Location Navig. Symp.*, Monterey, CA, USA, Apr. 23–26, 2018, pp. 374–381.

[32] P. Salvatori, C. Stallo, S. Pullen, S. Lo, and P. Enge
Use of SBAS corrections with local-area monitoring for railway guidance and control applications
In *Proc. IEEE ION Position, Location Navig. Symp.*, Monterey, CA, USA, Apr. 23–26, 2018, pp. 1379–1387.

[33] J. Lee, S. Pullen, and P. Enge
Sigma-mean monitoring for the local area augmentation of GPS
IEEE Trans. Aerosp. Electron. Syst., vol. 42, no. 2, pp. 625–635, Apr. 2006.

[34] J. Lee, S. Pullen, and P. Enge
Sigma overbounding using a position domain method for the local area augmentation of GPS
IEEE Trans. Aerosp. Electron. Syst., vol. 45, no. 4, pp. 1262–1274, Oct. 2009.

[35] J. Betz
Satellite-Based Augmentation Systems. New York, NY, USA: Wiley-IEEE Press, 2016.

[36] 2017. [Online]. Available: http://www.ersat-eav.eu/

[37] J. Marais, J. Beugin, and M. Berbineau
A survey of GNSS-based research and developments for the European railway signaling
IEEE Trans. Intell. Transp. Syst., vol. 18, no. 10, pp. 2602–2618, Oct. 2017.

[38] D. Lu and E. Schnieder
Performance evaluation of GNSS for train localization
IEEE Trans. Intell. Transp. Syst., vol. 16, no. 2, pp. 1054–1059, Apr. 2015.

[39] Report on the Eurocontrol XLS Business Case, European Air Traffic Management Programme, 2010.

[40] C. A. Brebbia, J. M. Mera, N. Tomii, and P. Tzieropoulos
COMPRAIL: Railway Engineering, Design and Operation. Ashurst, U.K.: WIT Press, 2017.

[41] P. Misra and P. Enge
Global Positioning System: Signals, Measurements, and Performance, 2nd ed. Warsaw, Poland: Ganga-Jamuna Press, 2010.

Cosimo Stallo (M'10) received the Ph.D. degree (*cum laude*) in microelectronics and telecommunications from the Electronic Department of Engineering, Faculty of University of Rome "Tor Vergata," Roma, Italy, in 2010.

From 2013 to 2014, he was a tutor for the course on communication systems with the University of Trento, Italy. Since 2012, he has been a Senior Researcher with RadioLabs Consortium, Rome, where he has been/is involved in the technical committees of different GNSS projects in the railway sector as ESA IAP 3InSat (Train Integrated Safety Satellite System), ESA IAP Space-Based Services for Railway Signalling, H2020 GSA ERSAT-EAV, and H2020 GSA Railway High Integrity Navigation Overlay System. Since 2011, he has been a Professor for the course on satellite navigation at Master of Science on "advanced satellite communication and navigation systems" with the University of Rome Tor Vergata. He is currently the Project Manager of ESA GSTP Element 2-Competiteveness Digital Beamforming for Rail. He is co-author of about 75 papers on international journals/transactions and proceedings of international conferences.

Dr. Stallo has been the Chair of the Space Systems Technical Panel of the IEEE AESS since February 2010.

Alessandro Neri (M'98) received the Doctoral degree in electronic engineering from "Sapienza" University of Rome, Rome, Italy, in 1977.

In 1978, he joined the Research and Development Department, Contraves Italiana S.p.A., where he gained a specific expertize in the field of radar signal processing and in applied detection and estimation theory, becoming the Chief of the advanced systems group. In 1987, he joined the INFOCOM Department, "Sapienza" University of Rome, as an Associate Professor in signal and information theory. In November 1992, he joined the Electronic Engineering Department, ROMA TRE University, as an Associate Professor in electrical communications, and became a Full Professor in telecommunications in September 2001. He is currently a Full Professor in telecommunications with the Engineering Department, ROMA TRE University, Rome. Since December 2008, he has been the President with the RadioLabs Consortium, Rome, a nonprofit Research Center created in 2001 to promote tight cooperation on applied research programs between universities and industries. His research interests include information theory, signal theory, signal and image processing, location and navigation technologies, and their applications to both telecommunications systems and remote sensing.

Pietro Salvatori received the first level degree in electronic engineering, the second level degree (*cum laude*) in information and communication technology engineering, and the Ph.D. degree in applied electronics from the University of Roma TRE, Rome, Italy, in 2010, 2013, and May 2017, respectively.

In 2013, he collaborated with RadioLabs consortium, Rome, carrying out research activities in the GNSS-based train control system. In January 2014, he joined the Ph.D. program in applied electronics with the University of Roma TRE obtaining the title in May 2017. He is currently with RadioLabs headquarter as a Satellite Navigation System Researcher.

Roberto Capua received the Master's degree in electronic engineering from University of Rome La Sapienza, Rome, Italy, in 1996.

He has a consolidated background in the field of GNSS applications research and development for public and private organizations. He worked on most important European commission programmes on Galileo design and applications. He was a Program Manager on satellite navigation applications for an important European satellite service provider. His areas of activity include advanced high-precision GNSS and augmentation systems, GNSS software receiver, and GNSS surveying for cadastral and mapping applications. He worked on the development of hardware and software navigation and communication technologies for road, inland waterway, aerospace, and surveying. He is currently responsible for GNSS R&D for Sogei, Rome, Italy, where he is managing a GNSS network for cadastral purposes and the GNSS SDR development project. He is furthermore delegate for his company in the Galileo Services Association and RTCM SC-104 Committee, where he chairs the Integrity Monitoring for High-Precision Application WG.

Francesco Rispoli received the Doctoral degree in electronic engineering from the Polytechnic of Turin, Turin, Italy, in 1978, and the Postgraduate Master degree in applied electromagnetism from the University La Sapienza, Rome, Italy, in 1980.

Since 2011, he has been involved in the innovation projects with the European Space Agency and the European GNSS Agency. He has chaired the Working Group for the satellite activities of the European Next-Generation Train Control System project with the rail and satellite stakeholders. In 2012, he launched with the Italian Railways Infrastructure as the Manager with the ERSAT pilot line with GNSS and satcom tested for integration into the ERTMS system. He is the Board Director with Galileo Services Association coordinating the satellite applications for rail. From 2005, he was the Chief New Initiatives with Telespazio and previously the Vice President Multimedia Business Unit with Alenia Spazio. In 2011, he joined Ansaldo STS, Genoa, Italy, where he is currently the Manager for train control system's satellite technology, and also the Director General with Radiolabs, Rome.

Dr. Rispoli received the Finmeccanica Innovation Prize and the Italian Prize of Prize with a satellite-based innovation for train control systems in 2012.